#### **Research Article**

Guoyu Li\* and Zekun Yin

# Low-carbon economic optimization of microgrid clusters based on an energy interaction operation strategy

https://doi.org/10.1515/nleng-2025-0134 received November 7, 2024; accepted April 10, 2025

Abstract: By optimizing energy utilization and integration, microgrids can improve the reliability of energy supply, reduce energy operating costs, and decrease energy emissions. However, there is insufficient coordination between energy interaction and low-carbon operation systems, resulting in increased carbon emissions and energy waste. Therefore, a low-carbon economic optimization method for microgrid clusters is built based on energy interaction operation strategies. This method adopts a multi-energy collaborative operation mode to construct a low-carbon optimization model for microgrid clusters. In the comparison of operating costs between microgrid clusters with and without energy interaction, for microgrids A, B, and C, when there was energy interaction, the operating costs of microgrids A and B both decreased by 25,400 RMB and 16,400 RMB, respectively, while the operating cost of microgrid C increased by 5,200 RMB. In terms of purchasing electricity costs, the purchasing electricity costs of microgrids A, B, and C all decreased in the energy interaction. In terms of purchasing gas costs, the purchasing cost of microgrid A slightly increased, while the purchasing cost of microgrids B and C decreased. Adopting energy interaction strategies has a positive effect on the economic cost of purchasing energy. After energy interaction, the purchasing demand of microgrid A was less than 4,000 kW, and most of the time, the purchasing energy demand was low. However, compared with before energy interaction, the purchasing demand of microgrids B and C significantly decreased. In the cost of carbon sales on microgrids, microgrids A, B, and C increased by \$213.73, \$230.02, and \$415.92, respectively, in scenarios 1–3. The designed method has a promoting effect on the comprehensive operational economy and low-carbon emissions of microgrid

clusters, providing technical references for the safety, stability, and environmental protection of microgrid clusters.

**Keywords:** energy interaction, microgrid cluster, low carbon economy, optimization, operation strategy

#### 1 Introduction

With the increasingly severe energy crisis and environmental issues, stable energy supply and energy conservation have become a global issue. The development and utilization of new energy technologies and small-scale power systems have also attracted widespread attention [1]. As a new distributed energy supply system, microgrids can integrate multiple energy sources and loads to achieve efficient utilization of energy. Various energy sources in microgrid systems are generally renewable, and the operational strategy of microgrids can achieve optimized energy allocation, thereby reducing energy waste, pollutant emissions, and lowering energy supply costs. Wind power and photovoltaic power generation have been widely used in renewable energy. Although they have advantages, their uncertainty and randomness have led to key safety, stability, and economic issues. The uncertainty of renewable energy and load demand has become a crucial issue, which has an obvious impact on the microgrid operation [2]. Multi-microgrid (MMG) systems are considered suitable candidates for wind power deployment. Although MMG systems can effectively utilize wind power generation, uncertainty and randomness still have impact on the scheduling and operation.

In response to the above issues and challenges, many scholars have carried out optimization research on microgrid energy operation. Chen *et al.* proposed a new cumulative relative regret decision method to optimize energy management, considering the inherent uncertainties associated with such systems. The traditional optimization model was enhanced by incorporating the demand response of heat load. The proposed method ensured the elasticity of

Zekun Yin: College of Economics, Bohai University, Jinzhou, 121000, China

<sup>\*</sup> Corresponding author: Guoyu Li, School of Business Administration, Liaoning Institute of Science and Engineering, Jinzhou, 121000, China, e-mail: GuoyuLiLq@outlook.com

microgrids, minimized the conservatism of microgrid operation, and verified its effectiveness [3]. To address the inherent uncertainty of wind power and implement an optimized scheduling strategy for MMG systems, Liu et al. proposed an adjustable robust optimization (ARO) based on meteorological clustering. This model performed well in improving the accuracy of wind power generation descriptions, enhancing cost-effectiveness, and declining carbon emissions [4]. Given the inevitable uncertainty brought by renewable energy and load demand, achieving reliable online energy dispatch for microgrid clusters has become challenging. To enhance privacy protection and overall convergence. Xie et al. proposed a decentralized decomposition and coordination approach on the basis of the multiplication alternating direction approach. A groundbreaking off-grid microgrid cluster energy management strategy on the basis of tubular model predictive control was designed [5]. To integrate demand response into the MMG based on renewable energy, Alamir proposed an improved algorithm to optimize energy management. The peak load reduction rate increased significantly from 13.9 to 16.13% without a hydrogen energy storage system, and from 12.68 to 16.46% with an integrated hydrogen energy storage system [6]. Fan et al. developed a deep lowcarbon economic optimization strategy for the integrated energy system (IES). The method considered carbon trading, coal consumption, penalties for renewable energy emission reductions, and natural gas costs. The method reduced carbon emissions and operating costs. Its performance was better than IES without CCUS, reducing costs by 8.8% and carbon emissions by 70.11% [7].

To address environmental pollution and conflicts of interest among multiple stakeholders in IES, Wang et al. built a new IES low-carbon economic collaborative optimization strategy on the basis of carbon trading mechanisms and Stackelberg game theory. The economic and environmental optimization scheduling of IES was achieved in a carbon-constrained environment [8]. Yan et al. established a bilateral distributed operation optimization model based on game theory. The experimental results confirmed that the economic benefits were enhanced, with power and heat loss rates of 0 and 0.00059%. The energy supply efficiency significantly enhanced, and the total carbon emissions declined by 8.64% [9]. The new energy used in the power grid declined carbon emissions. However, the output of wind power generation was unpredictable, which made it difficult to manage the power grid and increased the demand for carbon emission control. Yu et al. built a low-carbon economic dispatch strategy based on renewable energy and flexible resource cooperation. This strategy addressed the operational risk of wind power output randomness. The results verified its effectiveness

[10]. The complex market environment posed a serious challenge to the coordination of bidding strategies for multi-energy virtual power plant (MEVPP) between heterogeneous supply-side devices and demand-side users. In a recent publication, Wu et al. proposed a multi-objective MEVPP bidding strategy with different energy flows. Compared with the profit-oriented optimization, the multiobjective optimization with solutions led to a 46% decrease in profits and an 8% increase in satisfaction. Compared with a single-oriented optimization, a 5.2% decrease in satisfaction led to a profit increase of approximately 103% [11]. Yang et al. built an optimization scheduling model based on combined cooling, heating, and power generation and carbon capture devices, with the objective function of minimizing the total costs. A low-carbon and economical optimization scheduling model was developed based on the operational constraints of multiple energy flows in the IES. The total costs of hierarchical carbon trading were reduced by 5.9%, and the total operating costs were shorted by 3.1% [12]. The continuous advancement of renewable energy technologies has significantly increased the complexity and scale of power system architecture. To achieve low-latency data processing, emerging smart energy systems were usually deployed. This method ensured that microgrids made optimal cost control decisions under load balancing conditions. Therefore, Chen et al. proposed a twolayer optimization control model, which included an upper layer optimization control module and a lower layer optimization control module. The upper and lower modules worked together to provide information for system-wide decisionmaking. Subsequently, through a series of tests, the dual-layer optimization model was proven to be a feasible solution [13]. Domestic and foreign scholars have conducted extensive research on the energy operation optimization of microgrids. For example, the cumulative relative regret decision strategy proposed by Chen et al. enhanced the traditional microgrid energy management optimization model, improved system resilience, and reduced operational conservatism. Liu et al. effectively improved the accuracy of wind power generation description, enhanced cost-effectiveness, and reduced system carbon emissions through an ARO model based on meteorological clustering. In addition, the decentralized decomposition and coordination algorithm proposed by Xie et al., as well as the improved optimization algorithm proposed by Alamir solved the energy scheduling problem of microgrid clusters to some extent.

In summary, researchers have conducted some research on low-carbon economy optimization in microgrid clusters, including MMG systems, microgrid cluster energy management, and deep low-carbon economy optimization strategies. However, the application of energy interaction strategies to optimize the operation of microgrid clusters is not deep enough. Therefore, an innovative low-carbon economic optimization method for microgrid clusters based on energy interaction operation strategy is proposed to analyze energy interaction and multi-energy collaboration of microgrid wind and photovoltaic power generation, providing a technical basis for low-carbon economic optimization of microgrid clusters. An innovative optimization algorithm based on energy interaction operation strategy is designed, which innovatively comprehensively considers the energy demand, renewable energy output, and grid constraints of each microgrid in the microgrid cluster, achieving multi-energy coordinated operation. Therefore, in the field of microgrid optimization, this study provides new ideas and methods for microgrid optimization and provides a solid technical foundation for the low-carbon economic optimization of microgrid clusters.

The article structure of this study is as follows. The first section focuses on elaborating the process of the low-carbon economic optimization method for microgrid clusters based on energy interaction operation strategy, which is also the focus and innovation. The second section demonstrates the experimental verification. The third section draws conclusions and exhibits shortcomings and directions that need to be further explored in the future.

#### 2 Methods and materials

This study innovatively constructs a low-carbon economic optimization method for microgrid clusters based on an

energy interaction operation strategy. First, the microgrid energy interaction is achieved by combining an energy interaction operation strategy. Then, the multi-energy collaborative operation is adopted. A low-carbon economic optimization model for microgrid clusters is constructed.

### 2.1 Energy interaction operation strategy between microgrid clusters

Microgrid is an energy supply method based on small-scale energy systems, aimed at meeting the energy needs of specific regions or groups. It is composed of various sources, such as solar energy, wind energy, and traditional power networks [14,15]. In energy interconnection, the reliability and stability of the energy supply are crucial. This can be achieved by establishing an intelligent energy dispatch system. The intelligent energy dispatch system can monitor and control the generation and consumption of various energy sources in microgrids, meet user energy needs through reasonable energy resources, and ensure the normal operation [16,17]. Through energy interconnection, not only can the reliability of energy supply be improved, but also the operating costs can be reduced. Figure 1 displays the typical microgrid power supply architecture.

In Figure 1, the energy supply structure of microgrid clusters is mainly divided into energy production, conversion, storage, and utilization equipment. The main sources of energy supply are wind power generation, natural gas, and photovoltaic power generation [18]. However, there is currently insufficient cost optimization and energy synergy for

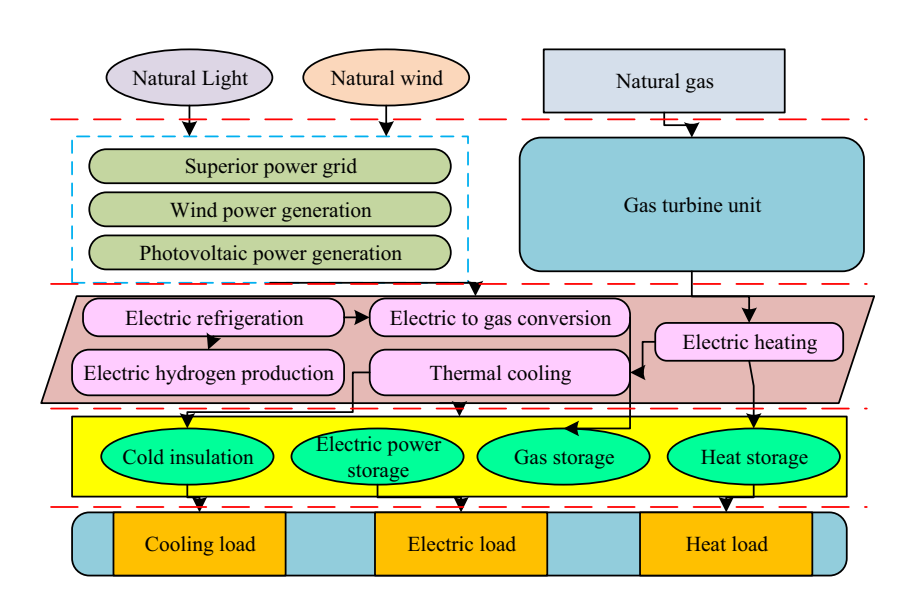


Figure 1: Microgrid cluster energy supply structure.

multi-energy supply. A low-carbon economic optimization method for microgrid clusters is built based on energy interaction operation strategies. The core of the energy interaction operation strategy between microgrids is to achieve efficient energy utilization and system stability by coordinating the supply and demand of different energy sources. Carbon trading price, abbreviated as carbon pricing, is a mechanism for clearly pricing greenhouse gas emissions in units of carbon dioxide equivalent per ton. At present, there are various forms of carbon pricing mechanisms in the industry, among which the most important are carbon emissions trading markets and carbon taxes. The carbon emissions trading market is a market-based energy-saving and emission reduction policy tool. Companies included in the carbon trading system need to set a unit carbon emission quota for every ton of carbon dioxide emitted. These companies can implement internal emission reduction measures to reduce emissions, obtain or purchase these quotas, or engage in quota trading with other companies. To achieve the stability and economy of microgrids, a distributed functional operating cost model is constructed based on multi-energy microgrid carbon trading and energy supply costs, combined with carbon emission trading schemes. Taking wind-solar units as an example, the schematic diagram is presented in Figure 2.

There are multiple forms of energy interaction and collaborative operation in multi-energy microgrid systems. An energy interaction strategy that considers multi-energy collaboration is proposed. Energy interaction can be divided into three types: decentralized, centralized, and mixed modes. The spatial position and collaboration of spatial interaction objects in multi-energy microgrid clusters are important parts of achieving energy interaction [19,20]. The centralized energy strategy refers to managing and allocating energy through a unified and centralized energy system. The decentralized energy strategy refers to dispersing energy facilities to multiple locations and

providing energy through a distributed energy system. The hybrid energy strategy refers to the optimization and combination of different types of energy to achieve complementarity and mutual promotion, and improve the stability and reliability of the overall energy system. In terms of cost reduction, centralized energy systems can purchase, store, and distribute energy on a large scale, thereby enjoying the cost reduction brought by economies of scale. Distributed energy systems can reduce energy losses during transmission, thereby improving energy utilization efficiency and reducing costs. The hybrid energy strategy can achieve complementarity between different types of energy, thereby optimizing the energy structure, improving energy utilization efficiency, and reducing costs. The spatial interaction structure of multi-energy microgrids is shown in Figure 3.

In the multi-energy collaboration between multienergy microgrid clusters, due to multiple microgrids, the ability of microgrids with energy interactions at all levels is optimized, as shown in the following equation:

$$R_{ex}^{k,t} = \sum_{k=1}^{k} X^{k,t} P_{e1, \text{int}}^{k,t} + \sum_{k=1}^{k} Y^{k,t} P_{e3, \text{int}}^{k,t} + \sum_{k=1}^{k} A^{k,t} P_{e1, \text{nei}}^{k,t} + \sum_{k=1}^{k} B^{k,t} P_{e3, \text{nei}}^{k,t}.$$
(1)

In Eq. (1), k represents a microgrid.  $A^{k,t}$  and  $B^{k,t}$  signify whether the microgrid participates in the first layer decision variable matrix.  $X^{k,t}$  and  $Y^{k,t}$  signify whether the microgrid participates in the second layer decision variable matrix.  $P_{e1,\, \rm int}^{k,t}$  and  $P_{e3,\, \rm int}^{k,t}$ , respectively, represent the interaction power matrix for the first layer energy interaction of the microgrid.  $P_{e1,\rm nei}^{k,t}$  and  $P_{e3,\rm nei}^{k,t}$ , respectively, represent the interaction power matrices for the second layer energy interaction of the microgrid. The expression of the above parameters is shown in the following equation:

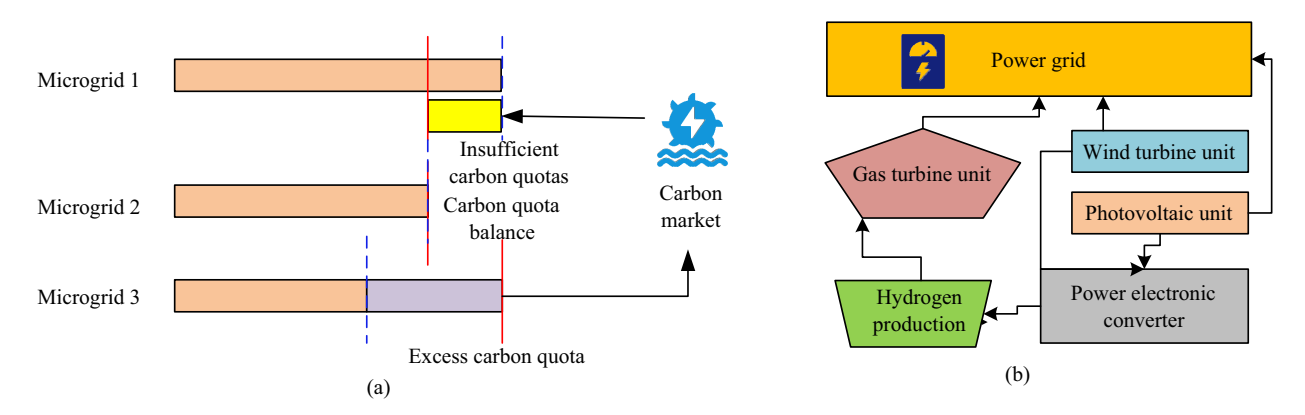


Figure 2: (a) Carbon emission trading. (b) Wind turbine energy supply - wind photovoltaic power generation for hydrogen production.

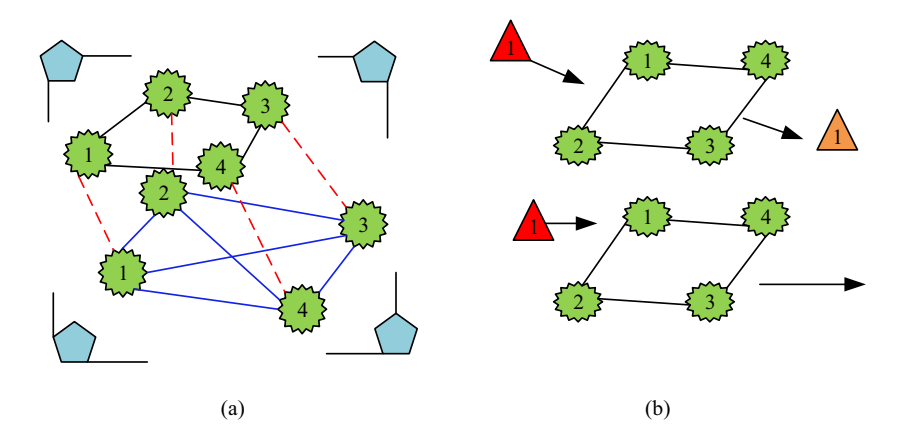


Figure 3: Multi-energy microgrid spatial interaction structure. (a) Microgrid space connection. (b) Microgrid space interaction.

$$\begin{aligned} P_{e1,\,\text{int}}^{k,t} &= [P_{e1,\,\text{int}}^{1,v,t}, \, ..., \, P_{e1,\,\text{int}}^{d,v,t}, \, ..., \, P_{e1,\,\text{int}}^{h,V_k,t}]^T \\ P_{e3,\,\text{int}}^{k,t} &= [P_{e3,\,\text{int}}^{1,v,t}, \, ..., \, P_{e3,\,\text{int}}^{g,v,t}, \, ..., \, P_{e3,\,\text{int}}^{G^h,V_k,t}]^T \\ P_{e1,\,\text{nei}}^{k,t} &= [P_{e1,\,\text{nei}}^{1,h,t}, \, ..., \, P_{e1,\,\text{nei}}^{d,h,t}, \, ..., \, P_{e1,\,\text{nei}}^{D^v,H_k,t}]^T \\ P_{e3,\,\text{nei}}^{k,t} &= [P_{e3,\,\text{nei}}^{1,h,t}, \, ..., \, P_{e3,\,\text{nei}}^{g,h,t}, \, ..., \, P_{e3,\,\text{nei}}^{g^v,H_k,t}]^T. \end{aligned} \tag{2}$$

In Eq. (2),  $H_k$  and  $V_k$ , respectively, represent a collection of microgrids with energy interaction behaviors directly connected to k and separated from k. h and v, respectively, represent a single microgrid directly connected to k. Among them,  $h \in H_k$ , and  $v \in V_k$ .  $D_{e1}$  represents the collection of power supply devices for microgrids.  $G_{e1}$  represents a collection of microgrid gas supply devices.  $d \in D_{e1}$  and  $g \in G_{e1}$ .  $D_{e1}^h$  and  $D_{e1}^v$  represent the distributed energy supply units and energy interaction sets of microgrids h and h, respectively. h0 and h1 and h2 and h3 and h4 and h5 and h6 and h7 and h8 and h9 an

$$\begin{cases} A^{k,t} = [a^{1,t} \quad a^{2,t} \quad \dots \quad a^{k,t}] \\ B^{k,t} = [b^{1,t} \quad b^{2,t} \quad \dots \quad b^{k,t}] \end{cases}$$

$$\begin{cases} a^{k,t} = \begin{cases} 1, P_{L,e1}^{k,t} - \sum_{d \in D^k} P_{e1}^{d,k,t} > 0 \\ 0, P_{L,e3}^{k,t} - \sum_{d \in D^k} P_{e3}^{d,k,t} > 0 \end{cases}$$

$$b^{k,t} = \begin{cases} 1, P_{L,e1}^{k,t} - \sum_{g \in G^k} P_{e1}^{g,k,t} > 0 \\ 0, P_{L,e3}^{k,t} - \sum_{g \in G^k} P_{e3}^{g,k,t} > 0. \end{cases}$$

$$(3)$$

In Eq. (3),  $a^{k,t}$  and  $b^{k,t}$  represent the decision variable elements in decision matrices  $A^{k,t}$  and  $B^{k,t}$ , respectively.  $P_e^{d,k,t}$ 

represents the power supply equipment inside k.  $P_{L,e1}^{k,t}$  represents the demand for electrical energy load. The second decision variable matrices are shown in the following equation:

$$V \begin{cases} X^{k,t} = [X^{1,v,t}, \dots, X^{d,v,t}, \dots, X^{D^{v},V_{k},t}] \\ Y^{k,t} = [y^{1,v,t}, \dots, y^{g,v,t}, \dots, y^{G^{v},V_{k},t}] \end{cases}$$

$$\begin{bmatrix} X^{d,v,t} = \begin{cases} 1, P_{e1}^{d,v,t} = \tau_{e1,\max}^{d,v,t} (P_{e1}^{k,t} - \sum P_{e1,\max}^{d,v,t} - \sum P_{e1,\max}^{d,v,t}) > 0, \tau_{e1,\max}^{d,v,t} \\ - \sum P_{e1,\max}^{d,h,t} > 0, \tau_{e1,\max}^{d,v,t} = (\tau|d \in D_{e1}^{v}, v \in V^{k}) \end{cases}$$

$$= (\tau|d \in D_{e1}^{v}, v \in V^{k})$$

$$0, \text{ otherwise}$$

$$\begin{cases} 1, P_{e3}^{g,v,t} = \tau_{e3,\max}^{d,v,t} (P_{e3}^{k,t} - \sum P_{e3,\max}^{g,v,t} - \sum P_{e3,\max}^{g,v,t}) > 0, \tau_{e3,\max}^{g,v,t} \\ - \sum P_{e3,\max}^{g,h,t} > 0, \tau_{e3,\max}^{g,v,t} > 0, \tau_{e3,\max}^{$$

In Eq. (4),  $x^{d,v,t}$  and  $y^{g,v,t}$ , respectively, represent the decision variable elements of the second-level decision matrix.  $\tau^{d,v,t}_{el,\max}$  and  $\tau^{g,v,t}_{e3,\max}$ , respectively, represent the maximum electrical energy interaction coefficient and maximum gas energy interaction supply coefficient provided by v spaced apart from k.  $P^{d,v,t}_{el}$  and  $P^{g,v,t}_{e3}$ , respectively, represent the electrical and gas energy interaction power of v in the second layer. In the third layer of decision variables, the ability flow equation is used to evaluate the stable state and energy trading [21]. Therefore, a multi-energy collaborative energy interaction strategy is proposed, as displayed in Figure 4.

In Figure 4, based on the above energy interaction strategy, a further optimization model for energy interaction between microgrid clusters is constructed, with the optimization objective of minimizing the operating costs of microgrids during the energy interaction process. The optimization model for energy interaction between microgrid clusters includes optimization functions and operating

constraints. The overall operating cost of the regional microgrid system includes the normal operating cost of the first layer multi-energy microgrid and the energy exchange cost between directly connected microgrids. The second layer is the energy exchange cost between microgrids and spaced microgrids. The energy purchase cost of the third layer multi-energy microgrid is the higher-level power grid and gas grid. The optimization model for energy interaction between multi-energy microgrids is shown in the following equation:

$$\min F = C_1 + C_2 + C_3. \tag{5}$$

In Eq. (5),  $C_1$ ,  $C_2$ , and  $C_3$ , respectively, represent the operating costs of the microgrid cluster, the energy interaction costs in the first and second layers, and the overall energy purchase costs of the microgrid cluster in the third layer. The constraints for the operation of microgrids include equality and inequality constraints. In the former, the balance of electrical power, power consumption, cold and hot power within the microgrid is crucial, as well as the overall balance of electrical power and power consumption within the microgrid cluster. The inequality constraints include distributed wind-photovoltaic unit coordinated operation, microgrid multi-energy operation

power variation, overall operating capacity of microgrid cluster, energy storage device operation, and energy operation cost constraints of microgrid cluster. In addition, there are other equipment operation constraints.

### 2.2 Low-carbon economic optimization operation model for microgrid clusters

Microgrids have the ability to operate independently and schedule autonomously, enabling energy interconnection and collaborative scheduling, and bringing new possibilities for energy supply. To achieve a low-carbon economy, a microgrid cluster energy interaction operation strategy is proposed, and a microgrid cluster low-carbon economy optimization operation model is further designed. Through the optimization algorithm, the optimal operation of the microgrid low-carbon economy is solved to achieve a microgrid low-carbon economy. Specifically, the study divides the model into upper-level economic optimization of microgrid clusters and lower-level economic optimization of microgrid clusters. To achieve multi-objective optimization of the economic optimization

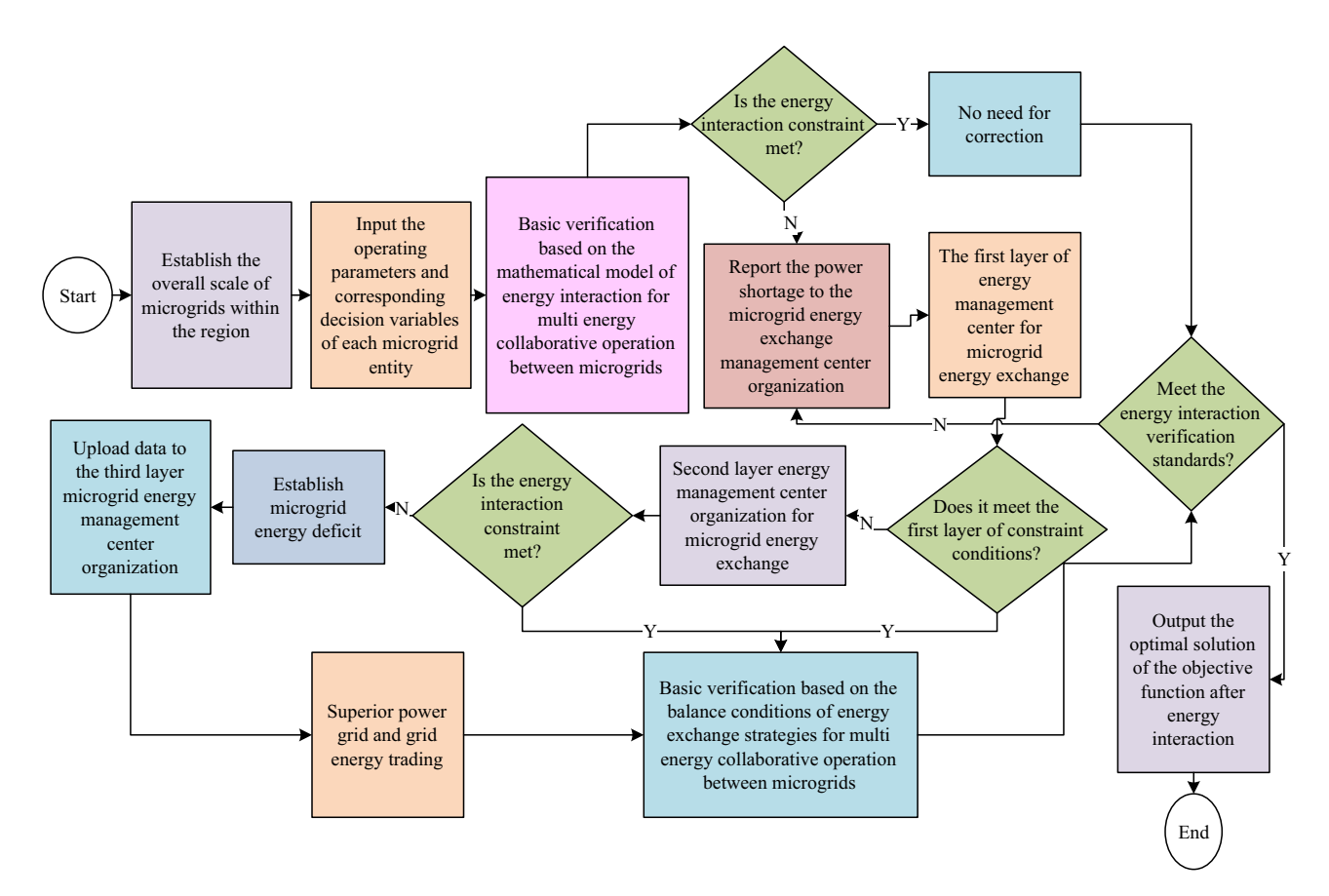


Figure 4: Energy interaction strategy based on multi-energy collaboration.

operation model and solve the upper and lower level models, a new particle swarm optimization (PSO) is combined, which has superior performance and is based on the improved niche technology [22,23]. The niche technology divides each generation into several classes, selects several individuals with high fitness from each class as excellent representatives of a class to constitute a group, and then hybridizes and mutates between populations to generate a new individual group. Simultaneously, pre-selection mechanism, exclusion mechanism, and sharing mechanism are applied to complete tasks [24-26]. This study combines the PSO algorithm with niche technology for solving multi-objective models. Meanwhile, the Pareto analysis method is introduced to describe the multi-objective optimization problem of microgrid clusters. First, a corresponding mathematical model is constructed, as shown in the following equation:

$$\min y = F(x) = (f_1(x), f_2(x), \dots, f_M(x))$$
s. t. 
$$\begin{cases} g_i(x) \le 0, & i = 1, 2, \dots, p \\ h_j(x) \le 0, & j = 1, 2, \dots, q. \end{cases}$$
(6)

In Eq. (6), y represents the target vector. x represents an N-dimensional decision vector. Y and X, respectively, represent the target space and decision space formed by

the two, and 
$$\begin{cases} y=(y_1,\ y_2,\ ...,\ y_M)\in Y\\ x=(x_1,\ x_2,\ ...,\ x_N)\in X \end{cases}.\ p \ \text{and}\ q \ \text{represent}$$

the number of equality and inequality constraints.  $g_i(x)$  and  $h_j(x)$ , respectively, signify the i-th inequality constraint and the j-th equality constraint. In this process, the Pareto front is taken to describe the multi-objective optimization problem, as shown in Figure 5.

If  $x_1$  Pareto dominates  $x_2$ , denoted as  $x_1 < x_2$ , the expression is shown in as follows:

$$\begin{cases} f_i(x_1) \le f_i(x_2), & \forall i \in \{1, 2, ..., M\} \\ f_j(x_1) \le f_j(x_2), & \exists j \in \{1, 2, ..., M\}. \end{cases}$$
 (7)

In Eq. (7),  $x_1$  and  $x_2$  signify the two solutions of Eq. (6). The optimization objective of the upper-level economic optimization part is to minimize the comprehensive operating cost and minimize the fluctuation of communication power between the overall microgrid cluster and the upper-level power grid [27]. Under the proposed energy exchange strategy between multiple energy microgrids, energy transactions are conducted with the higher-level energy backbone network based on the overall energy shortage and energy surplus within the cluster area. The cost of purchasing and selling electricity and natural gas is allocated based on the weight of the energy demand share of each sub-microgrid within the cluster. The mathematical model is shown in the following equation:

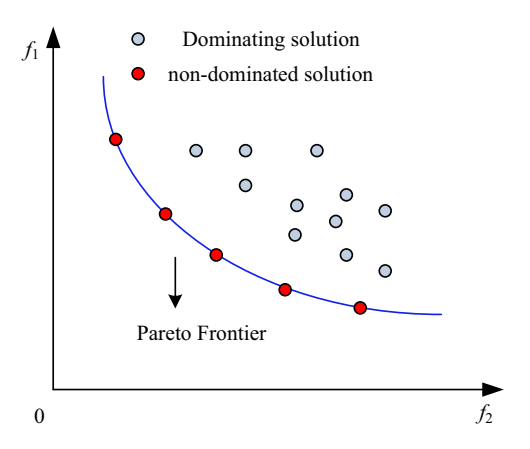


Figure 5: Multi-objective solving problem: Pareto frontier.

$$C = \min \sum_{t=1}^{T} \sum_{i=1}^{n} (C_{i,\text{grid},t} + C_{i,\text{gas},t} + C_{i,\text{toc},t}).$$
 (8)

In Eq. (8), C signifies the overall operating cost of a microgrid cluster running for a certain period of time.  $C_{i,\text{grid},t}$  and  $C_{i,\text{gas},t}$  signify the electricity and gas costs of the microgrid cluster and the primary energy grid of the previous level. i represents a microgrid cluster.  $C_{i,\text{toc},t}$  signifies the overall operating costs of i. In the latter objective, there are voltage frequency oscillations and power fluctuations at the access points during the energy interaction between microgrid clusters, which increase network losses and operating costs. Therefore, the objective is shown in the following equation:

$$\begin{cases} P_E = \min \left\{ \sum_{t=1}^{T} (P_{\text{gride }1,t} - P_{\text{agride }1,t})^2 / T \right\} \\ P_{\text{gride }1,t} = \begin{cases} P_{i,\text{buye }1,t_i}; \text{ Cluster purchasing status} \\ P_{i,\text{selle }1,t_2}; \text{ Cluster energy sales status.} \end{cases}$$
 (9)

In Eq. (9),  $P_E$  represents the power fluctuation in energy trading communication between the microgrid cluster and the upper-level main power grid.  $P_{\text{gride 1},t}$  represents the actual value of the corresponding communication power.  $P_{\text{agride 1},t}$  represents the corresponding average communication power.  $P_{i,\text{buye 1},t_i}$  and  $P_{i,\text{selle 1},t_2}$ , respectively, represent the actual communication power values for purchasing and selling energy in microgrid clusters. The power balance constraint between the regional microgrid cluster system and the higher-level power grid is shown in the following equation:

$$\begin{cases} P_{i,\text{ree } 1,t} < P_{i,\text{coe } 1,t} < P_{i,\text{nee } 1,t} \\ P_{j,\text{coe } 1,t} - P_{j,\text{pcoe } 1,t} = P_{j,\text{nee } 1,t} \\ \sum_{i=1}^{n} P_{i,\text{nee } 1,t} = P_{\text{gride } 1,t} + \sum_{i=1}^{n} P_{i,\text{coe } 1,t}. \end{cases}$$
(10)

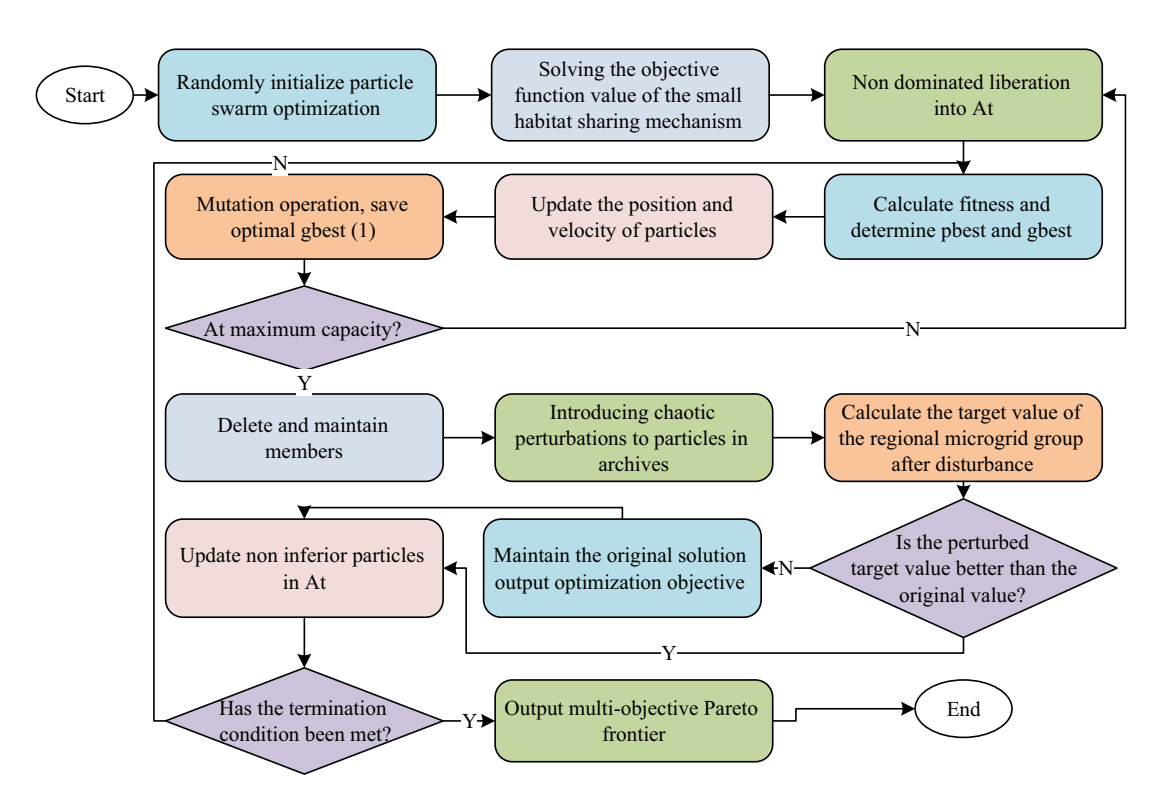


Figure 6: New PSO algorithm solving process.

In Eq. (10), i and j represent microgrid clusters. t represents time.  $P_{i,\text{ree }1,t}$  and  $P_{j,p\cos }1,t$ , respectively, represent the power shortage and balance of two microgrid clusters.  $P_{i,\cos }1,t$  and  $P_{j,\cos }1,t$ , respectively, represent the electrical power output of two microgrid clusters.  $P_{i,\text{nee }1,t}$  and  $P_{j,\text{nee }1,t}$  represent the total power demand of two microgrid clusters. The power balance constraint between the regional microgrid cluster system and the higher-level gas grid is shown in the following equation:

$$\begin{cases} P_{i,\text{ree } 3,t} < P_{i,\text{coe } 3,t} < P_{i,\text{nee } 3,t} \\ P_{j,\text{coe } 3,t} - P_{j,\text{pcoe } 3,t} = P_{j,\text{nee } 3,t} \\ \sum_{i=1}^{n} P_{i,\text{nee } 3,t} = P_{\text{gride } 3,t} + \sum_{i=1}^{n} P_{i,\text{coe } 3,t}. \end{cases}$$
(11)

In Eq. (11),  $P_{i,\text{ree }3,t}$  and  $P_{j,p\cos }3,t$  represent the shortage and balance of gas power in two microgrid clusters.  $P_{i,\cos }3,t$  and  $P_{j,\cos }3,t$ , respectively, represent the electrical power output of two microgrid clusters.  $P_{i,\text{nee }3,t}$  and  $P_{j,\text{nee }3,t}$  represent the total demand for gas power of two microgrid clusters. Similarly, the lower microgrid cluster is to minimize the average operating costs and achieve the highest wind-photovoltaic efficiency. The mathematical model for the previous objective (minimum average operating cost) is shown in the following equation:

In Eq. (12),  $C_{i,\mathrm{all},\mathrm{CO}_2}$  signifies the total carbon trading cost of i.  $C_{i,\mathrm{buy}\ gj,t}$  and  $C_{i,\mathrm{sell}\ gj,t}$  represent the costs of purchasing and selling gas when i interacts with j.  $\bar{C}_{\mathrm{run},t}$  signifies the average operating cost of a microgrid cluster.  $C_{i,\mathrm{run},t}$  signifies the operating costs of the i-th microgrid.  $C_{i,\mathrm{buy}\ ej,t}$  and  $C_{i,\mathrm{sell}\ ej,t}$  represent the cost of purchasing and selling electricity when i interacts with j. The mathematical expression for the latter goal (highest wind photovoltaic efficiency) is shown in the following equation:

$$\eta_{\rm wp} = \frac{\sum_{i=1}^{n} (P_{i,\rm WT,t} + P_{i,\rm PVT,t})}{\sum_{i=1}^{n} (P_{i,\rm WT,z,t} + P_{i,\rm PVT,z,t})}.$$
 (13)

In Eq. (13),  $\eta_{\rm wp}$  represents the wind-photovoltaic efficiency factor.  $P_{i,{\rm WT},t}$  signifies the actual consumption of wind power by microgrids.  $P_{i,{\rm PWT},t}$  signifies the photovoltaic power generation.  $P_{i,{\rm WT},t}$  represents the total power that wind power can generate.  $P_{i,{\rm PWT},t}$  represents the total power that can be generated by photovoltaics. Constraints include carbon trading cost constraints, energy interaction and transmission constraints between microgrids, power balance constraints, *etc.* The carbon trading cost constraint is presented in the following equation:

$$-0.5C_{i,\text{toc},t} \le C_{i,\text{all},\text{CO}_2} \le 0.5C_{i,\text{toc},t}.$$
 (14)

$$\bar{C}_{\text{run},t} = \frac{\min \sum_{i=1}^{n} (C_{i,\text{all},\text{CO}_2} + C_{i,\text{run},t} + \sum_{j=1}^{n-1} C_{i,\text{buy }ej,t} + C_{i,\text{buy }gj,t} - C_{i,\text{selle }j,t} - C_{i,\text{sell }gj,t})}{n}.$$
(12)

In Eq. (14),  $C_{i,\text{toc},t}$  represents the overall operating cost. The constraints of energy interaction and transmission between microgrids, as well as power balance constraints, are expressed as shown in the following equation:

$$\begin{cases} P_{\min}^{ij} < P_t^{ij} < P_{\max}^{ij} \\ \Delta P_{\min}^{ij} < P_t^{ij} - P_{t-1}^{ij} < \Delta P_{\max}^{ij} \end{cases} \\ P_{\text{MEG } i,t} + P_{i,\text{buy } e1,t} - P_{i,\text{sell } e1,t} + \sum_{j=1}^{n-1} P_{i,t}^{ji} - \sum_{j=1}^{n-1} P_{j,t}^{ij} \end{cases}$$

$$= L_{e1}^{i,t}.$$
(15)

In Eq. (15),  $P_{\max}^{ij}$  and  $P_{\min}^{ij}$ , respectively, signify the upper and lower boundaries of the power interaction between i and j energy in the overall microgrid cluster.  $\Delta P_{\max}^{ij}$  and  $\Delta P_{\min}^{ij}$  signify the upper and lower boundaries of the power interaction between i and j energy.  $P_{\text{MEG}\ i,t}$  is the total output of each device in i.  $P_{i,t}^{ij}$  and  $P_{i,t}^{ji}$  represent the energy transferred between i and j, respectively. Finally, a new PSO is applied to solve the optimization model, as shown in Figure 6.

In Figure 6, At represents the external archive size. pbest and gbest represent the individual and global optimal positions of the initial position, respectively. First, the particle swarm is initialized, and the objective function is solved using the niche technique. The non-dominated solution set (NDSS) is added to the external archive. Then, the fitness is calculated to determine pbest and gbest. The particle velocity and position are updated, and the optimal gbest is saved through the mutation operation. Whether the maximum capacity has

been reached is judged. If not, the steps of adding the NDSS to the external archive are repeated until the maximum capacity is reached. Then, members are deleted and maintained, chaotic perturbations are added to particles in At, and the perturbed microgrid cluster target value is calculated. It is judged whether the target value after disturbance is better than the original value. If it is better than the original value, the non-inferior particles in the scale are updated. If not, the optimization objective is output as the original solution. The non-inferior particles in the scale are output. Finally, whether the termination condition is satisfied is judged. If it satisfies, the multi-objective Pareto front is output. If not, the above steps are repeated [28–30]. Based on the above analysis, a microgrid cluster optimization method based on energy interaction operation strategy is built, as presented in Figure 7.

In Figure 7, the operational data of the microgrid cluster corresponding to the input is solved using a novel PSO. During this process, the parameters and objectives of the microgrid cluster, including wind power, photovoltaic, and load demand, are optimized. Finally, the optimal solution obtained by the optimization model is output.

In terms of convergence speed, the proposed PSO divides the optimization problem into multiple sub-problems and runs a PSO on each sub-problem. Moreover, multiple groups are searched in parallel. Each group is independent and can transmit information, which helps the algorithm to locate the global optimal solution faster and accelerate the convergence process. In terms of computational efficiency, the fast convergence property is utilized for global search in the early stages

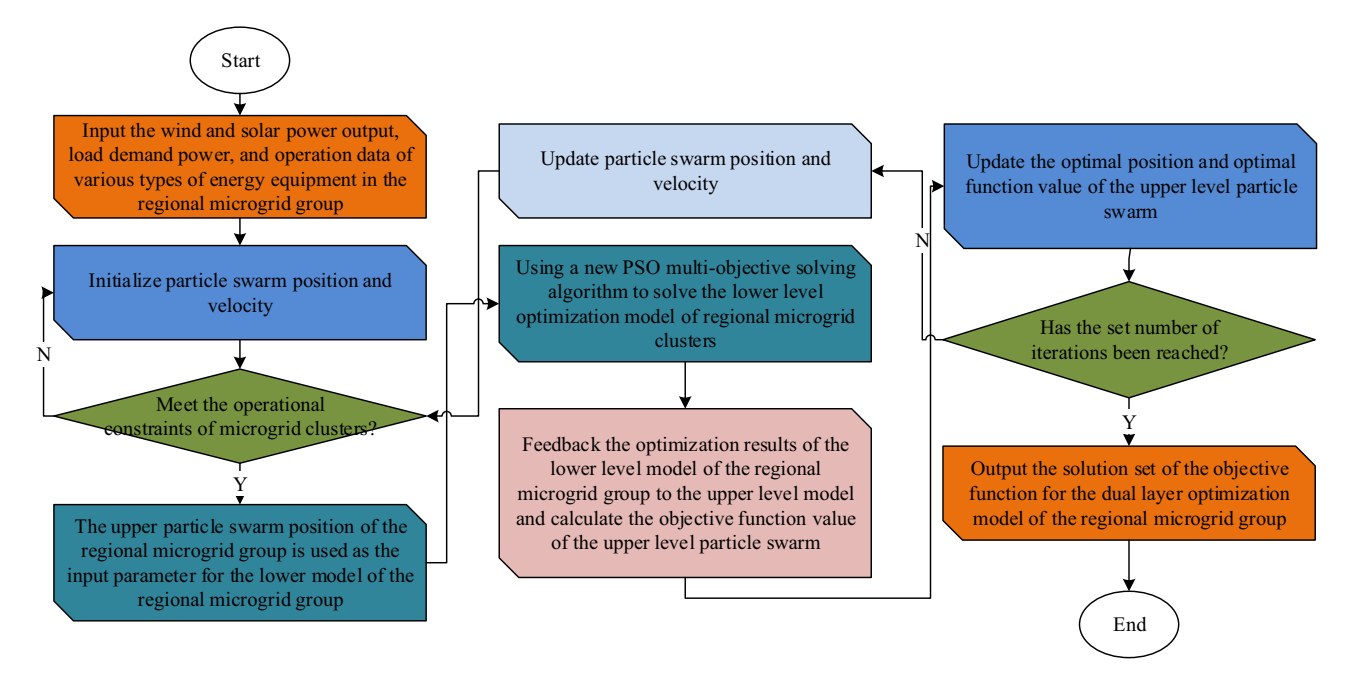


Figure 7: Double-layer optimization process diagram for a microgrid cluster.

of PSO, while a fine search strategy is adopted in the later stages to improve the quality of the solution. This combination helps to improve overall computational efficiency.

To address the scalability limitations of the current framework, modular design principles are adopted in practical applications, where microgrids and energy types are designed and implemented as independent modules. New microgrids and energy types can be easily added to the system as new modules. Unified interface standards and protocols are developed to ensure interoperability and compatibility between different microgrids and energy types, simplify system integration processes, and reduce maintenance costs. High-performance computing technologies such as distributed computing, cloud computing, etc., are utilized to improve the data processing capability and communication speed of the system. The above methods can solve the scalability problem of larger networks for different energy sources.

#### 3 Results

To validate the low-carbon economic optimization method for microgrid clusters based on the energy interaction operation strategy proposed in the research; an experiment is conducted to verify it. The corresponding design parameters and experimental data results are analyzed, and the advantages and feasibility are verified.

## 3.1 Preparation and data statistics for the low-carbon optimization verification experiment of microgrid cluster energy interaction

The experimental simulation environment used in the study is Matlab software, version 3.6.0. Matlab, as a

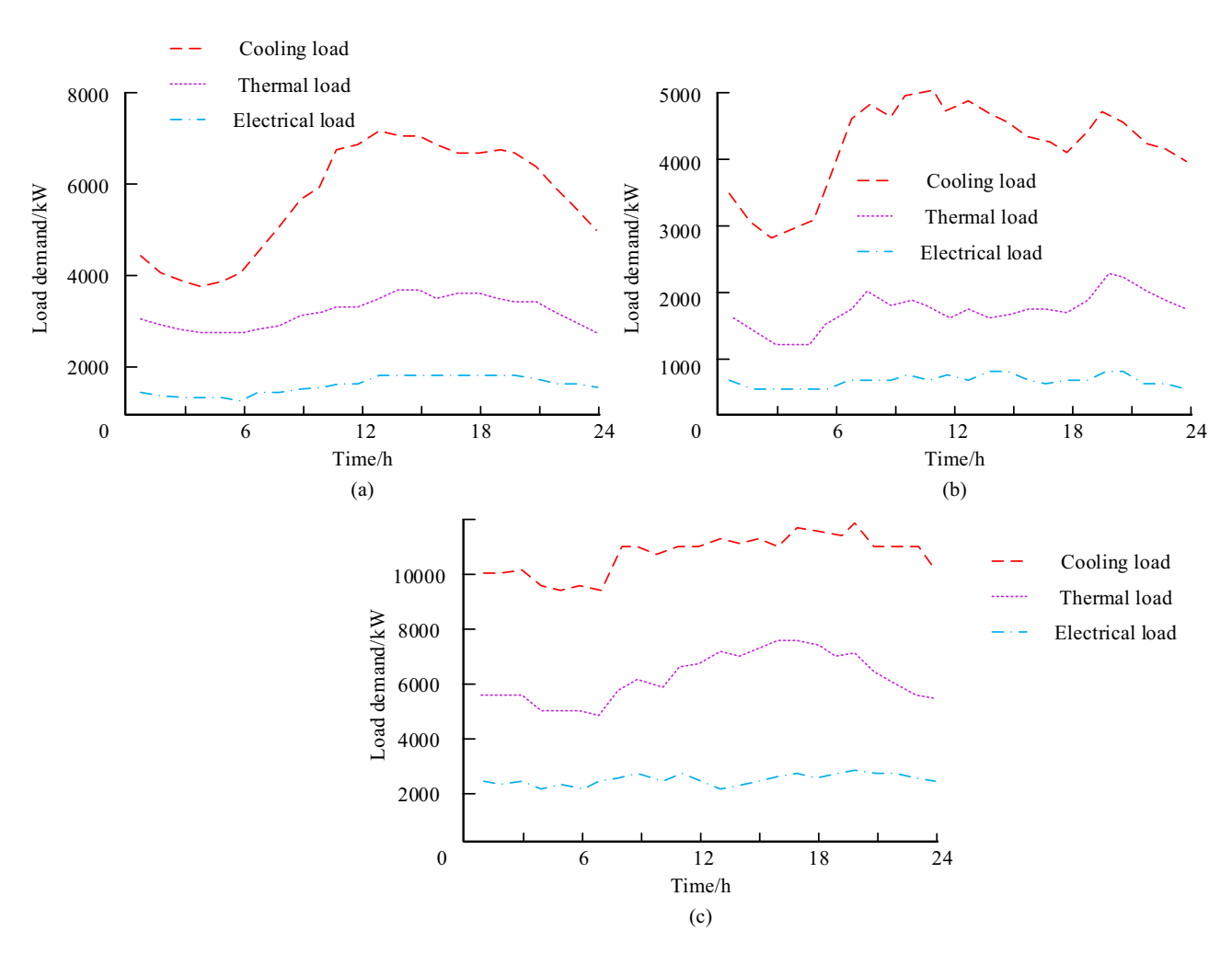


Figure 8: Three microgrid cooling, thermal, and electrical load demands: (a) Micronet A, (b) Micronet B, and (c) Micronet C.

powerful simulation tool, has broad application prospects in carbon trading and microgrid simulation. Through reasonable configuration and optimization, the advantages of Matlab in simulation analysis can be fully utilized, providing strong support for scientific research and engineering applications. This article selects three multi-energy microgrids in a certain region of Northeast China as example objects. An energy transfer example system composed of an IEEE37 node distribution system and an eightnode natural gas system is used to simulate and verify the energy interaction strategy between multi-energy microgrids. The selected multi-energy microgrids A, B, and C are all microgrids containing load types such as electricity, heat, and cooling. Decision variables for each type of energy conversion device are selected based on the actual energy conversion process within the microgrid. The specific demand is displayed in Figure 8. Microgrids A, B, and C had the smallest electrical load demand and the largest cooling load demand. Microgrid A had higher wind and solar power output, and the variation ranges of cooling load, thermal load, and electrical load were around 3,800-5,000 kW, 2,800-3,200 kW, and 1,000 kW, respectively, providing energy in energy interaction. The cooling load demand of microgrid B was particularly high, while the electrical load demand and thermal output were relatively small, with variation ranges of 2,700-5,000 kW and 500-1,000 kW, respectively. The cooling, thermal, and electrical load demands of microgrid C were all high, with varying ranges of 10,000 kW and above, 5,000-8,000 kW, and 2,000-3,000 kW, respectively.

To effectively explore the process and optimization effect of microgrid energy interaction, the experimental

statistics of the power supply and output of distributed wind and photovoltaic generators in three microgrids are shown in Figure 9. From Figure 9(a), microgrid A had a larger distributed wind power supply, followed by microgrid B, with a supply and output of less than 5 MW. Microgrid C had the smallest supply and output, which was below 4 MW. In Figure 9(b), the output of photovoltaic generators in three microgrids is further analyzed. The photovoltaic generator in microgrid A had the highest output, reaching around 4 MW, while microgrids B and C had outputs of around 3 and 2.9 MW. Overall, microgrid A exhibits strong energy supply capabilities in both distributed wind and photovoltaic power generation, with good energy interaction and supply performance. Microgrids B and C are relatively weak on energy supply and output, but still have certain potential for wind and photovoltaic utilization.

## 3.2 Optimization analysis of energy interaction and low-carbon economy in microgrid clusters

Table 1 displays the operating costs between microgrid clusters with and without energy interaction behavior. For microgrids A, B, and C, when energy interaction existed, the operating costs of microgrids A and B both decreased by 25,400 RMB and 16,400 RMB, respectively, while the operating cost of microgrid C increased by 5,200 RMB. In terms of purchasing electricity costs, the purchasing electricity costs of microgrids A, B, and C all

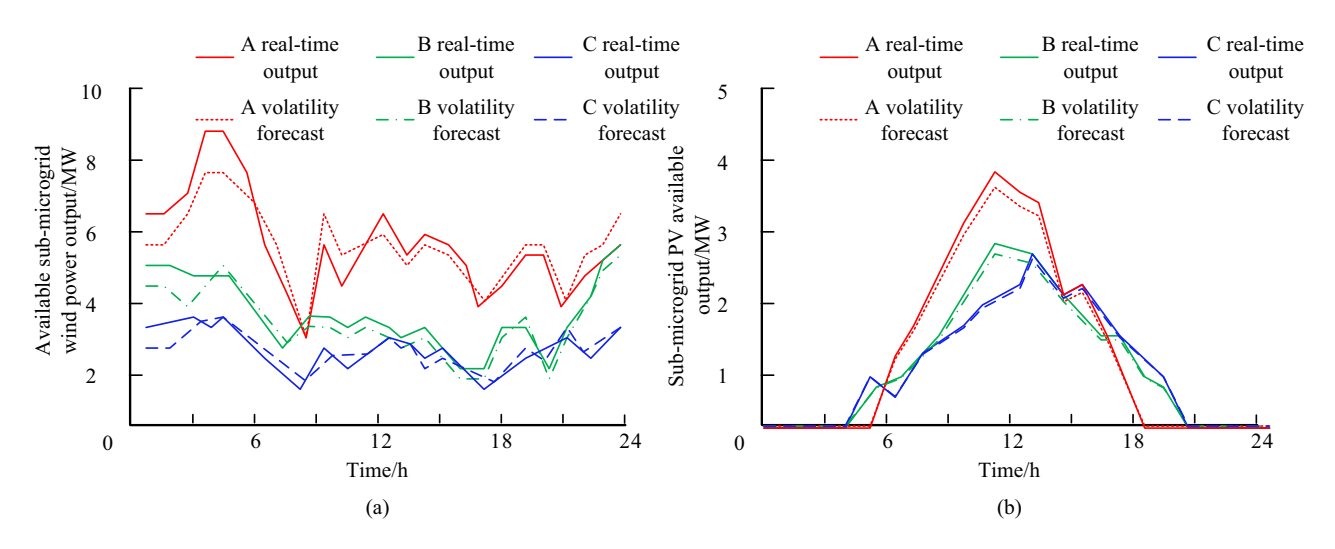


**Figure 9:** The power supply and output of distributed wind and photovoltaic generators in three microgrids. (a) Energy microgrids wind turbine output. (b) Energy microgrid photovoltaic genset output.

Table 1: Operating costs between microgrid clusters with and without energy interaction behavior

Cost type	No energy interaction/ 10,000 RMB	There is an energy interaction between microgrids/10,000 RMB	
A operating cost	14.89	12.35	
B operating costs	15.84	14.20	
C operating costs	16.12	16.64	
Cost of purchasing electricity for A	5.92	4.69	
Cost of purchasing electricity for B	5.29	4.45	
Cost of purchasing electricity for C	6.77	4.98	
Purchase cost of gas A	3.61	3.96	
Purchase cost of gas B	4.21	3.79	
Purchase cost of gas C	5.13	3.87	
A Energy interaction cost	0	2.17	
B Energy interaction cost	0	1.95	
C Energy interaction cost	0	2.11	
Total operating cost	77.78	75.16	

decreased in the presence of energy interaction. In terms of purchasing gas costs, the purchasing costs of A microgrid slightly increased, while the purchasing costs of microgrids B and C decreased. Adopting the energy interaction strategy has a positive effect on the economic costs of purchasing energy.

Figure 10 shows the impact of carbon trading prices on the optimized operation of microgrid clusters and the results of microgrid energy interaction. Figure 10(a) shows the operational impact. As the carbon trading price increased, energy costs gradually rose. The carbon trading cost increased before 18\$  $t^{-1}$  and then gradually decreased to \$0. The total cost increased before the price reached 36\$  $t^{-1}$  and then gradually decreased. Figure 10(b) shows the energy interaction results of microgrids. After energy interaction among these three microgrids, microgrid A

provided energy to microgrids B and C during other peak operating periods, optimizing the overall operational stability of the microgrid cluster.

Figure 11 shows the changes in energy purchase demand before and after energy interaction in the energy microgrid. In Figure 11(a), before energy interaction, the minimum purchase time for energy demand in microgrid A was 12:00, with a purchase demand of 0 kW. During other time periods, the purchasing demand was also lower at 22:00 and 24:00, with a maximum value of 10 h and a purchasing demand of 4,000 kW. Similarly, the minimum energy demand of microgrid B was at 2:00, 4:00, 24:00, and the highest was at 14 h. The minimum purchase energy demand time for microgrid C was at 2:00, 4:00, and 24:00, and the maximum purchase demand was around 6,000 kW. Overall, the three microgrids have a higher

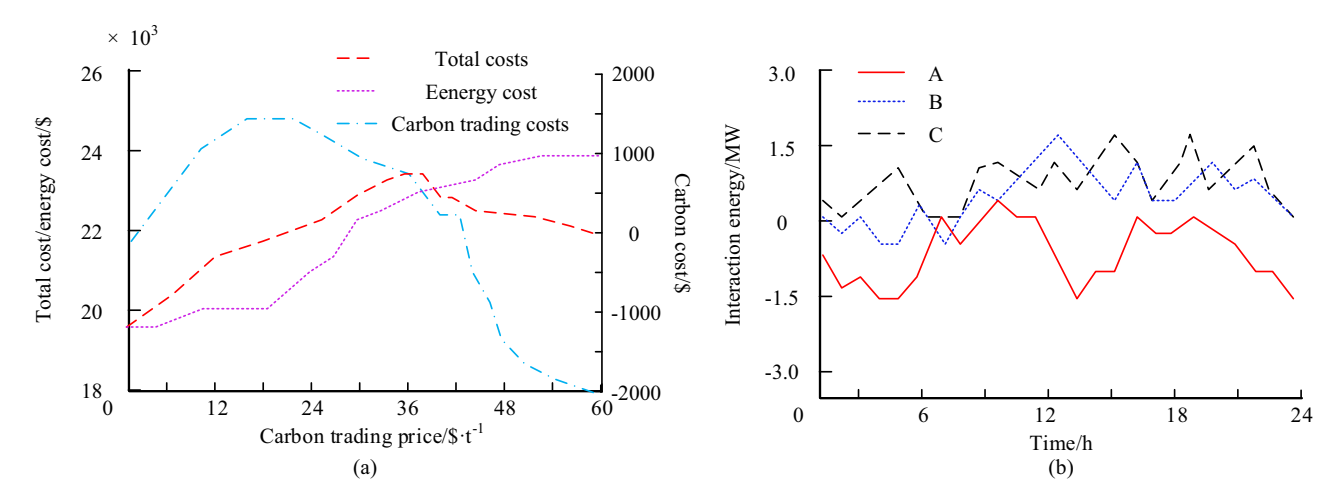


**Figure 10:** The impact of carbon trading prices on the optimized operation of microgrid clusters and the results of microgrid energy interaction. (a) The operational impact. (b) The energy interaction results of microgrids.

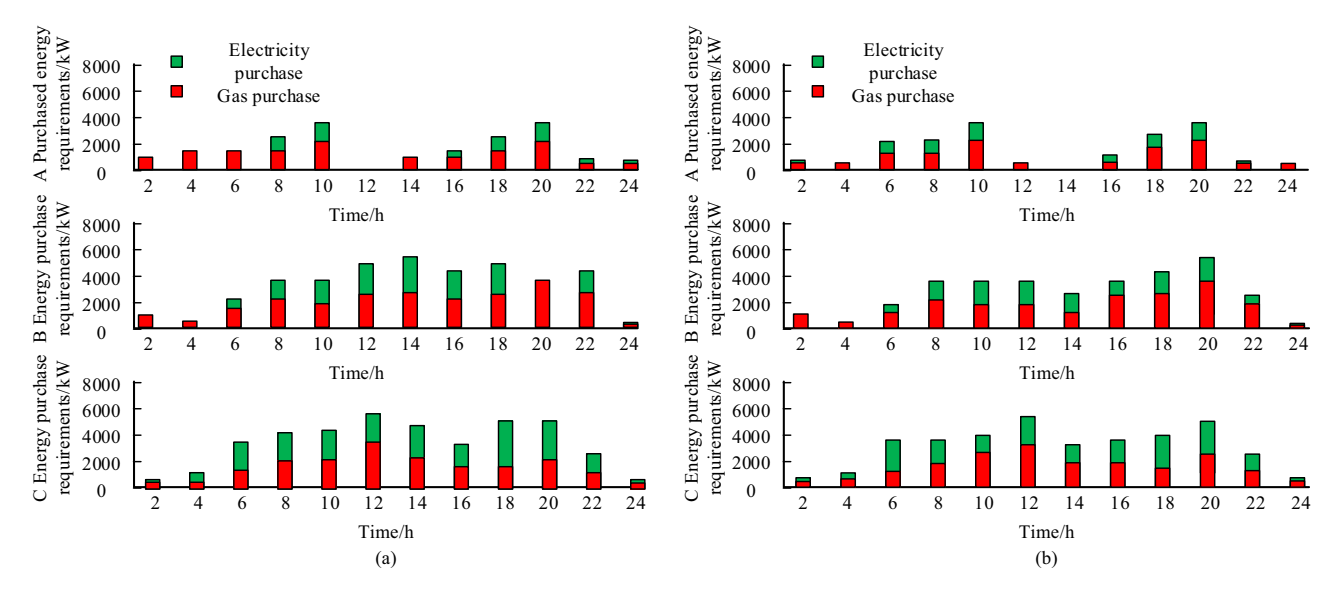


**Figure 11:** Changes in energy purchase demand before and after energy interaction in energy microgrids. (a) Demand for micro-networked energy purchases. (b) Demand for energy purchases following energy interactions between microgrids.

demand for purchasing energy during the day time. In Figure 11(b), after energy interaction, the purchasing demand of microgrid A was less than 4,000 kW, and most of the time, the purchasing energy demand was low. However, compared with before energy interaction, the purchasing demand of microgrids B and C significantly decreased. After energy interaction, the purchase of electricity and gas energy has decreased, indicating that adopting an energy interaction operation strategy has a promoting effect on the decrease in purchasing demand.

Table 2 shows the operating carbon trading costs of microgrids in three scenarios. In terms of carbon emissions, scenario 1 had the highest carbon emissions of 62.55 tons, indicating that the energy use or production process of microgrid clusters in this scenario was relatively environmentally unfriendly. Scenario 3 further reduced the carbon emissions of the microgrid cluster to 42.45 tons, with the lowest emissions. This indicated that the microgrid cluster achieved better results in environmental

protection. In the carbon cost of micro online shopping, the difference in carbon cost between micro networks A, B, and C in scenarios 1–3 was \$85.45, \$36.14, and \$59.96, respectively. The cost of microgrid A increased while the cost of other micro networks decreased. In the cost of carbon sales on microgrids, microgrids A, B, and C increased by \$213.73, \$230.02, and \$415.92, respectively, in scenarios 1–3, indicating that the carbon revenue was highest in scenario 3.

Figure 12 shows the iteration results of the upper and lower layers of the microgrid cluster. In Figure 12(a), at iterations of 60 and 90, the results were close, and the Pareto front was closest to the optimal value. As the overall operating cost increased, the communication power of the microgrid decreased to 1,000 W. In Figure 12(b), at iterations of 60 and 90, the Pareto front was closest to the optimal value. As the operating cost increased, the proportion of wind photovoltaic efficiency increased to 80%. The research has achieved the optimization goal of minimizing

 Table 2: Carbon trading costs of microgrid operation in three scenarios

Scenario	Scenario 1	Scenario 2	Scenario 3
Cluster carbon emissions (t)	62.55	46.93	42.45
Carbon purchase cost of microgrid A (\$)	90.31	112.52	175.76
Carbon purchase cost of microgrid B (\$)	245.98	223.86	209.84
Carbon purchase cost of microgrid C (\$)	298.21	276.92	238.25
Cost of selling carbon on microgrid A (\$)	168.12	252.63	381.85
Cost of selling carbon on microgrid B (\$)	134.77	315.20	364.79
Cost of selling carbon on microgrid C (\$)	66.34	332.67	482.26

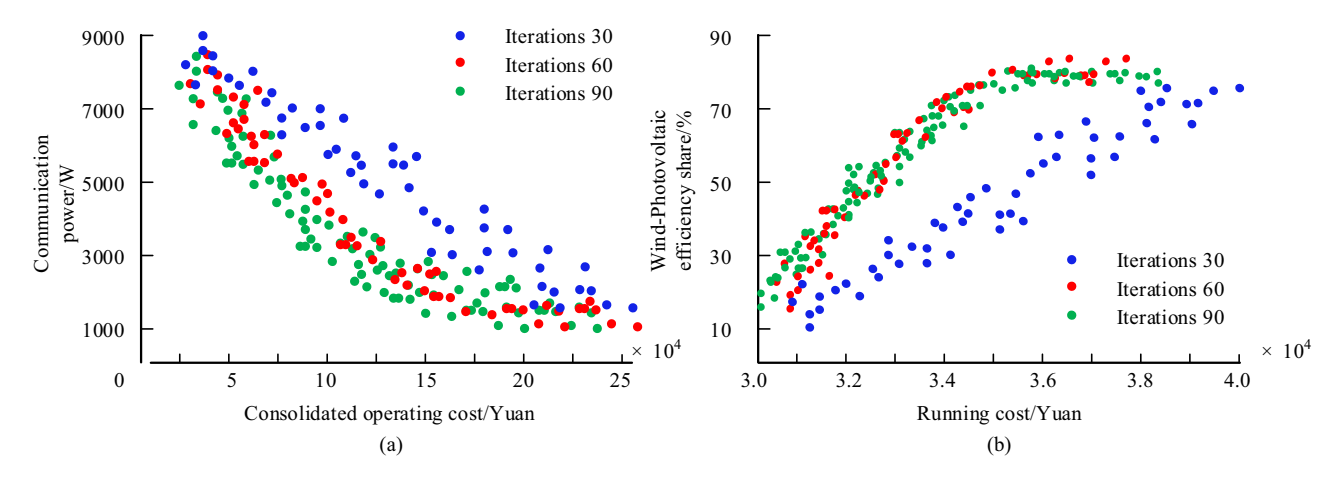


**Figure 12:** Optimization iteration results of upper and lower layers of the microgrid cluster. (a) Microgrid cluster upper layer optimization objective Pareto. (b) Microgrid cluster lower layer optimization objective Pareto.

communication power and maximizing wind-photovoltaic efficiency.

To effectively and accurately evaluate the low-carbon economic optimization operation model of microgrid clusters, the Pareto optimal solution for the comprehensive operation cost of communication power fluctuation, wind and solar efficiency, and operation cost is shown in Figure 13. In Figure 13(a), from Group 1 to Group 5, the fluctuation of communication power gradually increased, and the average fluctuation of communication power in Group 30 was 3,247. From Group 1 to Group 5, the comprehensive operating cost gradually decreased, with an average comprehensive operating cost of 154,114 RMB for Group 30. In Figure 13(b), from Group 1 to Group 5, the proportion of wind and solar efficiency gradually increased, indicating that the utilization efficiency of wind and solar gradually improved.

The average wind and solar efficiency ratio of the 30 groups was 91.17%, which was a relatively high level. From Group 1 to Group 5, the operating costs gradually increased, indicating that as the wind and solar efficiency improved, the operating costs also increased. The average operating cost for Group 30 was 32,569 RMB. Overall, the solution of Group 3 is the optimal one, which can achieve a low-carbon economy and stable operation of microgrid clusters.

#### 4 Discussion and conclusion

In energy interconnection, reasonable energy allocation can ensure the normal operation of microgrids. In addition, energy interconnection can improve the reliability of

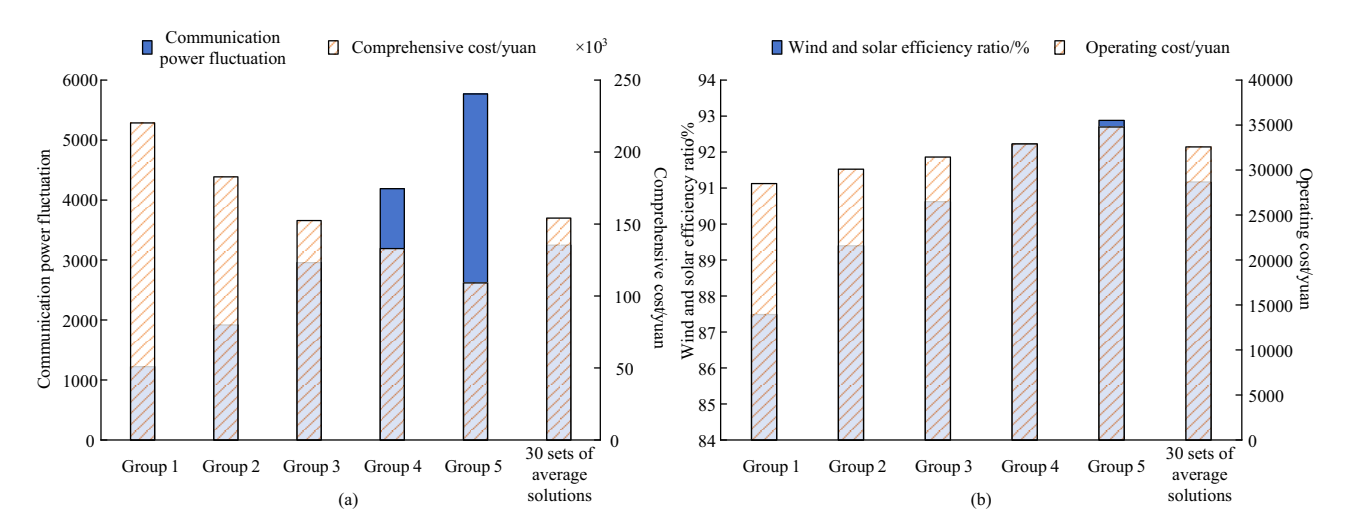


**Figure 13:** Pareto optimal solution for comprehensive operating cost, wind and solar efficiency, and operating cost of communication power fluctuation. (a) Communication power and comprehensive cost. (b) Wind and solar efficiency ratio and operating costs.

the energy supply and also reduce the operating costs. A low-carbon economic optimization method for microgrid clusters based on energy interaction operation strategy was proposed. As the carbon trading price increased, energy costs gradually rose. The carbon trading cost increased before 18\$ t<sup>-1</sup> and then gradually decreased to \$0, while the total cost increased before the price reached 36\$ t<sup>-1</sup> and then gradually decreased. After the carbon trading price reached a certain level, the carbon trading cost gradually decreased to zero, and the total cost also began to decrease, achieving effective control of energy costs. In the energy interaction results of microgrids, microgrid A provided energy to microgrids B and C during other peak operating periods, optimizing the overall operational stability of the microgrid cluster. The average communication power fluctuation was 3,247, and the average operating cost was 32,569 RMB, which achieved a lowcarbon economy and stable operation of microgrid clusters. At iterations of 60 and 90, the Pareto frontier of microgrid communication power and wind-photovoltaic efficiency ratio was closest to the optimal value. As the overall operating cost of microgrids increased, the microgrid communication power decreased to 1,000 W, and the wind-photovoltaic efficiency ratio increased to 80%. By analyzing the communication power of microgrids and the proportion of wind photovoltaic efficiency under different iterations, the Pareto front closest to the optimal value was found, providing strong support for minimizing communication power and maximizing wind photovoltaic efficiency. The research has achieved the optimization goal of minimizing communication power and maximizing wind-photovoltaic efficiency. A low-carbon economic optimization method for microgrid clusters based on energy interaction operation strategy was proposed, providing a new theoretical perspective and solution for the rational allocation of energy resources in microgrids in energy interconnection. The research results can be directly applied to the design and optimization of microgrids and energy interconnection systems, which can help improve the reliability of energy supply, reduce operating costs, and achieve low-carbon economic goals. Optimizing energy exchange strategies can help promote the openness and competition of the energy market and facilitate the development and application of clean energy. Although this study has achieved significant results, there is still insufficient consideration in various aspects of energy interaction processes such as interruption and termination. This discovery provides new directions and challenges for subsequent research, which will help further improve and optimize the design and operation strategies of microgrids and energy interconnection systems.

**Funding information:** The research is supported by the development path of Specialized, Refined, Differentiate, and Innovative enterprises with small and medium size in Jinzhou, General Project of Liaoning Provincial Department of Education (No. LJKMR20221940). General Project of Liaoning Provincial Department of Education, SSDN enterprises (Specialized, Sophisticated, Distinctive, Novel) drive intelligent transformation, digitalization, and networking for high-quality development of Liaoning's manufacturing sector, (No. LJ112513217001).

**Author contributions:** All authors have accepted responsibility for the entire content of this manuscript and approved its submission.

**Conflict of interest:** Authors state no conflict of interest.

Data availability statement: All data generated or analyzed during this study are included in this published article.

#### References

- Yu Z, Dou Z, Zhao Y, Xie R, Qiao M, Wang Y, et al. Grid scheduling strategy considering electric vehicles participating in multimicrogrid interaction. J Electr Eng Technol. 2023;18(3):1557-72. doi: 10.1007/s42835-022-01294-x.
- Zhang Z. Optimization of operation strategy of multi-islanding microgrid based on double-layer objective. Energies. 2024;17(18):4614-5. doi: 10.3390/en17184614.
- [3] Chen T, Cao Y, Qing X, Zhang J, Sun Y, Amaratunga GAJ. Multi-energy microgrid robust energy management with a novel decision-making strategy. Energy. 2022;239(15):1-11. doi: 10.1016/j.energy.2021.121840.
- Liu Y, Li X, Liu Y. A low-carbon and economic dispatch strategy for a multi-microgrid based on a meteorological classification to handle the uncertainty of wind power. Sensors. 2023;23(11):5350. doi: 10. 3390/s23115350.
- Xie P, Jia Y, Chen H, Wu J, Cai Z. Mixed-stage energy management [5] for decentralized microgrid cluster based on enhanced tube model predictive control. IEEE Trans Smart Grid. 2021;12(5):3780-92. doi: 10.1109/TSG.2021.3074910.
- Alamir N. Optimizing two-stage energy management in renewable-[6] based multi-microgrid using a modified student psychology-based optimization with demand response and hydrogen storage. Int J Hydrogen Energy. 2024;63(1):696-719. doi: 10.1016/j.ijhydene.2024.
- Fan J, Zhang L, Yuan R, Yan W, Zhao N, Nim N. Deep low-carbon economic optimization using CCUS and two-stage P2G with multiple hydrogen utilizations for an integrated energy system with a high penetration level of renewables. Sustainability. 2024;16(13):5722. doi: 10.3390/su16135722.
- [8] Wang R, Cheng S, Zuo X, Liu Y. Optimal management of multi stakeholder integrated energy system considering dual incentive demand response and carbon trading mechanism. Int I Energy Res. 2022;46(5):6246-63. doi: 10.1002/er.7561.

- [9] Yan Y, Liu M, Li S, Li C, Li K, Wang X. Distributed low-carbon operational optimization model of an integrated energy system based on ladder carbon trading and integrated demand response. Int J Green Energy. 2024;21(6):1324–44. doi: 10.1080/15435075. 2023.2251048.
- [10] Yu G, Zhang Z, Li X, Shen L, Yan H, Cui G, et al. Low-carbon economic dispatching strategy based on feasible region of cooperative interaction between wind-storage system and carbon capture power plant. Renew Energy. 2024;228:120706. doi: 10.1016/ j.renene.2024.120706.
- [11] Wu QL, Li C, Bai J. Optimal bidding strategy for multi-energy virtual power plant participating in coupled energy, frequency regulation and carbon trading markets. Int J Hydrogen Energy. 2024;73(7):430–42. doi: 10.1016/j.ijhydene.2024.06.067.
- [12] Yang P, Jiang H, Liu C, Kang L, Wang C. Coordinated optimization scheduling operation of integrated energy system considering demand response and carbon trading mechanism. Int J Electr Power Energy Syst. 2023;147:108902. doi: 10.1016/j.ijepes.2022. 108902.
- [13] Chen Y, Hayawi K, Fan M, Chang SY, Tang J, Yang L, et al. A bilevel optimization model based on edge computing for microgrid. Sensors. 2022;22(20):7710. doi: 10.3390/s22207710.
- [14] Wang S, Tan Q, Ding X, Li J. Efficient microgrid energy management with neural-fuzzy optimization. Int J Hydrogen Energy. 2024;64(15):269–81. doi: 10.1016/j.ijhydene.2024.03.291.
- [15] Huangfu Y, Tian C, Zhuo S, Li P, Quan S, Zhang Y, et al. An optimal energy management strategy with subsection bi-objective optimization dynamic programming for photovoltaic/battery/ hydrogen hybrid energy system. Int J Hydrogen Energy. 2023;48(8):3154–70. doi: 10.1016/j.ijhydene.2022.10.133.
- [16] Nasiri T, Moeini-Aghtaie M, Azimi FM. Energy optimization of multicarrier energy systems to achieve a low carbon community. J Clean Prod. 2023;390:136154. doi: 10.1016/j.jclepro.2023.136154.
- [17] Lan J. Research on multi-microgrid electricity-carbon collaborative sharing and benefit allocation based on emergy value and carbon trading. Electronics. 2024;13(17):3394. doi: 10.3390/ electronics13173394.
- [18] Yang A, Wang H, Tan LZ. Capacity optimization of hybrid energy storage system for microgrid based on electric vehicles' orderly charging/discharging strategy. J Clean Prod. 2023;411(20):1–21. doi: 10.1016/j.jclepro.2023.137346.
- [19] Chen H, Yang S, Chen J, Wang X, Li Y, Shui S, et al. Low-carbon environment-friendly economic optimal scheduling of multi-energy

- microgrid with integrated demand response considering waste heat utilization. J Clean Prod. 2024;450:141415. doi: 10.1016/j. jclepro.2024.141415.
- [20] Azaroual M, Mbungu NT, Ouassaid M. Toward an intelligent community microgrid energy management system based on optimal control schemes. Int J Energ Res. 2022;46(15):21234–56. doi: 10.1002/er.8343.
- [21] John N, Janamala V, Rodrigues J. An adaptive inertia weight teaching-learning-based optimization for optimal energy balance in microgrid considering islanded conditions. Energy Syst. 2024;15(1):141–66. doi: 10.1007/s12667-022-00526-3.
- [22] Dong H, Fu Y, Jia Q, Zhang T, Meng D. Low carbon optimization of integrated energy microgrid based on life cycle analysis method and multi time scale energy storage. Renew Energy. 2023;206:60–71. doi: 10.1016/j.renene.2023.02.034.
- [23] García A, Monsalve-Serrano J, Villalta D, Guzmán-Mendoza M. Optimization of low carbon fuels operation on a CI engine under a simplified driving cycle for transportation de-fossilization. Fuel. 2022;310(15):122338. doi: 10.1016/j.fuel.2021.122338.
- [24] Guo X, Wang X, Wu X, Chen X, Li Y. Carbon emission efficiency and low-carbon optimization in Shanxi Province under "dual carbon" background. Energies. 2022;15(7):2369. doi: 10.3390/en15072369.
- [25] Xie X, Fu H, Zhu Q, Hu S. Integrated optimization modelling framework for low-carbon and green regional transitions through resource-based industrial symbiosis. Nat Commun. 2024;15(1):3842. doi: 10.1038/s41467-024-48249-6.
- [26] Zhang Y, Cheng V, He SG. A model-adaptive clustering-based time aggregation method for low-carbon energy system optimization. IEEE Trans Sustain Energy. 2023;14(1):55–64. doi: 10.1109/TSTE. 2022.3199571.
- [27] Wu H, Wang S. Design and optimization of intelligent orchard frost prevention machine under low-carbon emission reduction. J Clean Prod. 2023;433:139808. doi: 10.1016/j.jclepro.2023.139808.
- [28] Xiang Y, Wu G, Shen X, Ma Y, Gou J, Xu W. Low-carbon economic dispatch of electricity-gas systems. Energy. 2021;226:120267. doi: 10.1016/j.energy.2021.120267.
- [29] Liu C, Wang H, Wang ZY, Liu Z, Tang Y, Yang S, et al. Research on life cycle low carbon optimization method of multi-energy complementary distributed energy system: A review. J Clean Prod. 2022;336(15):130138. doi: 10.1016/j.jclepro.2022.130380.
- [30] Ari I. A low carbon pathway for the Turkish electricity generation sector. GLCE. 2023;1(3):147–53. doi: 10.47852/ bonviewGLCE3202552.